


Steplike spectral distribution of photoelectrons at the percolation threshold in heavily *p*-doped GaAsS. V. Poltavtsev ^{1,2,*}, R. I. Dzhirov,³ V. L. Korenev,³ I. A. Akimov ^{1,3}, D. Kudlacik,¹ D. R. Yakovlev ^{1,3} and M. Bayer^{1,3}¹*Experimentelle Physik 2, Technische Universität Dortmund, 44221 Dortmund, Germany*²*Spin Optics Laboratory, St. Petersburg State University, 198504 St. Petersburg, Russia*³*Ioffe Institute, Russian Academy of Sciences, 194021 St. Petersburg, Russia*

(Received 7 August 2019; revised 28 June 2020; accepted 30 June 2020; published 13 July 2020)

The origin of the steplike shoulder on the high-energy side of the low-temperature photoluminescence spectrum of heavily *p*-doped GaAs is studied experimentally. It is shown that it is controlled by both the Fermi-Dirac distribution of the holes and the energy distribution of the photoexcited electrons exhibiting a sharp steplike dependence. The latter results from abrupt changes in the energy relaxation rate at the percolation threshold separating localized from delocalized electron states. A comprehensive set of optical techniques based on spin orientation of electrons, namely, the Hanle effect, time- and polarization-resolved photoluminescence, as well as transient pump-probe Faraday rotation, are used for these studies. Two different electron ensembles with substantially different lifetimes of 20 and 280 ps are identified. Their spin relaxation times are longer than 2 ns, so that the spin lifetime is limited by the electron lifetime. The relative contribution of short- and long-lived photoexcited electrons to the emission spectrum changes abruptly at the step in the high-energy photoluminescence tail. For energies above the percolation threshold, the electron states are empty due to fast energy relaxation, while for lower energies the relaxation is suppressed and the majority of photoelectrons populates the states located there.

DOI: [10.1103/PhysRevB.102.014204](https://doi.org/10.1103/PhysRevB.102.014204)**I. INTRODUCTION**

In a high-purity semiconductor, such as epitaxially grown GaAs, the light absorption is dominated by the narrow resonant line of the excitons, which remain free even at liquid-helium temperatures. When, however, the crystal is doped to a sufficiently high concentration of impurities, the absorption line broadens [1]. The reason is that the high-impurity density disturbs the translational crystal symmetry by introducing disorder. As a result, the carrier momentum conservation law is not strictly fulfilled and optical transitions that are indirect in **k** space become possible. This unavoidably leads to a broadening of the sharp spectral features in photoluminescence (PL) and PL excitation (PLE) spectra.

There are several remarkable phenomena that take place in systems with strong disorder. For example, the conductivity increases rapidly in a steplike way when continuously increasing the charge carrier density, which is known as metal-insulator transition [2]. In detail, this steplike behavior takes place due to the existence of the percolation threshold, which separates localized and delocalized states in the energy spectrum [2,3]. The percolation threshold exists in the empty band within the single-particle Anderson model [3]. Another prominent example for a steplike behavior in a disordered system is the quantum Hall effect, which manifests itself by steps in the Hall resistance when scanning the external magnetic field [4]. These steps appear due to the presence of disorder. A further remarkable phenomenon, which occurs in the case of strong acceptor doping of direct band-gap semiconductors, is

the appearance of a sharp edgelike shoulder in the high-energy flank of the PL spectrum at low temperatures [5,6]. So far, it has been associated with the formation of a Fermi-Dirac distribution of the holes in the valence/acceptor band and the sharpness of this edge has been believed to reflect the hole temperature [7].

However, the Fermi level of the holes alone is insufficient to explain the appearance of the sharp low-temperature PL edge in a heavily *p*-doped crystal because the indirect optical transitions in momentum space should inevitably lead to broadening of the step. An additional condition for the distribution of the photoexcited electrons in the conduction band has to be introduced therefore.

In this study we demonstrate that this additional condition is dictated by a sharp steplike electron distribution function. The energy where the step occurs corresponds to the percolation threshold in the conduction band. For energies larger than the percolation threshold, the electron states are not occupied due to their fast energy relaxation. For lower energies the relaxation is suppressed and most of the photoexcited electrons populate energy states just below the percolation threshold. Two important features of these observations deserve particular attention. First, the population of electrons is not described by a Fermi-Dirac distribution because the photoexcited electrons are not in equilibrium. Second, the statistics is far from being degenerate since the population of localized states in the conduction band is significantly smaller than unity, also for the electrons with energy below the percolation threshold. This is because the density of photoexcited electrons in typical PL experiments is about 10^{13} – 10^{14} cm⁻³, which is significantly smaller than the concentration of donors

*sergei.poltavtcev@tu-dortmund.de

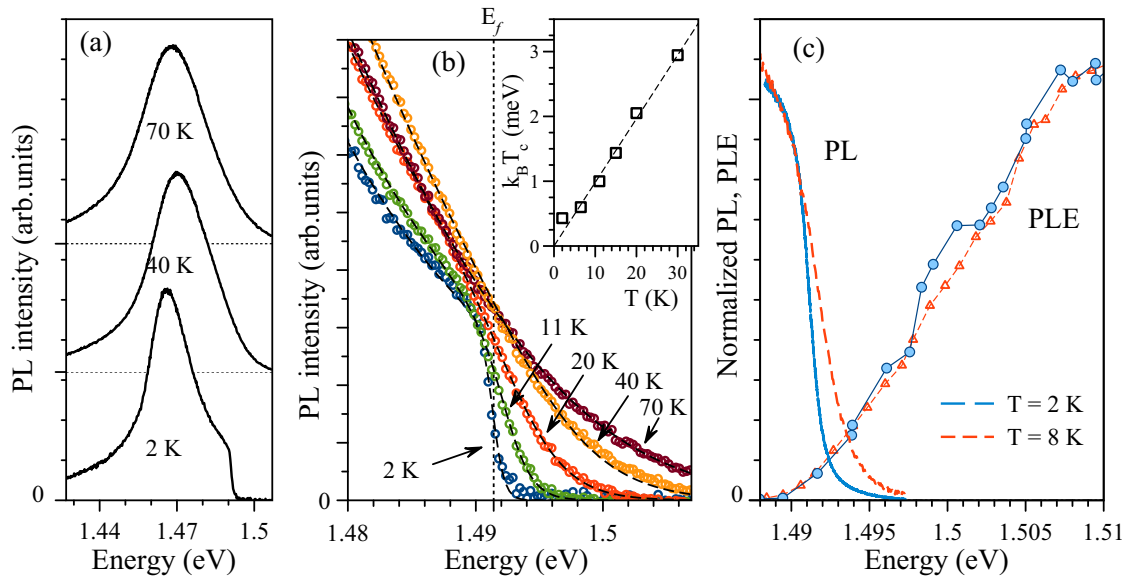


FIG. 1. PL and PLE spectroscopy of p -doped GaAs with acceptor density $N_A = 5 \times 10^{18} \text{ cm}^{-3}$: (a) PL spectra for different temperatures, shifted vertically for clarity. (b) Softening of the step on the high-energy side of the PL spectrum with rising sample temperature. Circles are experimental data; dashed lines are fits with Eq. (1). Inset shows the temperature dependence of the thermal energy $k_B T_c$ characterizing the spectral width of the PL steplike edge. Dashed line is linear fit for $T > 6 \text{ K}$. (c) Comparison of normalized PL (solid and dashed lines) and PLE (circles and triangles) spectra measured at $T = 2$ and 8 K . The PLE detection energy is 1.467 eV .

of 10^{17} cm^{-3} , which are present due to compensation related to the growth.

We use a set of optical techniques based on optical orientation of electrons in semiconductors [8] to study the dynamics of photoexcited electrons in a highly p -doped GaAs crystal. Using the Hanle effect, i.e., the depolarization of the PL in a transverse magnetic field, we evaluate the spin lifetime, which undergoes drastic changes at photon energies close to the sharp PL edge. Using time-resolved PL and pump-probe Faraday rotation we monitor the spin dynamics and evaluate the population and spin relaxation times of the electrons at different energies. At low temperatures, strong changes of the electron lifetime for photon energies around the high-energy PL edge evidence the existence of sharp steplike distribution function in the vicinity of a percolation threshold for the photoexcited electrons in the conduction band.

The paper is organized as follows. First, the properties of low-temperature PL and sharp edge in the high-energy tail of PL spectrum are presented. Then, the Hanle effect is studied in two ranges of magnetic field strengths. Further, the kinetics of the photoexcited carriers and of their spins is studied by time-resolved PL followed by a comprehensive discussion and resulting conclusions.

II. EXPERIMENTAL RESULTS

A. Samples and photoluminescence

The main studied sample (AH4227) is a $25\text{-}\mu\text{m}$ GaAs layer which was heavily p doped by Ge with a concentration of $N_A = 5 \times 10^{18} \text{ cm}^{-3}$, grown by metal-organic chemical vapor deposition (MOCVD). The GaAs layer is separated from the GaAs substrate by a $2\text{-}\mu\text{m}$ -thick $\text{Al}_{0.3}\text{Ga}_{0.7}\text{As}$ barrier layer. A $2\text{-}\mu\text{m}$ -thick cap layer of $\text{Al}_{0.3}\text{Ga}_{0.7}\text{As}$ was deposited on

top of the structure. Additionally, a similar structure (R94-1) with the acceptor concentration of $N_A = 3 \times 10^{18} \text{ cm}^{-3}$ was investigated.

A set of PL spectra measured at temperatures $T = 2\text{--}70 \text{ K}$ under cw-laser excitation with 1.55-eV photon energy is shown in Fig. 1(a). The broad PL, even at low temperatures, features a characteristic sharp edge on the high-energy side. This observation is in excellent correspondence with PL spectra of heavily p -doped GaAs, reported previously by other authors [5,6,9,10]. The spectrum's shape does not change with increasing excitation density up to at least 30 W cm^{-2} for a laser spot diameter of about $100 \mu\text{m}$. The excitation density in most cw experiments reported here was less than 10 W cm^{-2} and therefore below this value. Increasing the sample temperature results in a smoothing of the PL edge, as seen from Fig. 1(b). The shape of the edge can be fitted well with the following empirical function based on the Fermi-Dirac distribution:

$$y(E) \sim e^{-E/E_W} / (e^{(E-E_f)/k_B T_c} + 1). \quad (1)$$

Here, $E_f \approx 1.4914 \text{ eV}$ represents an energy gap, which is weakly affected by temperature up to 30 K ; k_B is the Boltzmann constant, and $E_W = 0.016 \pm 0.002 \text{ eV}$ ($T = 2\text{--}30 \text{ K}$) is a fit parameter describing the high-energy PL profile below the sharp edge. We attribute this decay to a smooth change of the density of states with increasing photon energy. The fitted effective temperature T_c is in fairly good correspondence with the lattice temperature. Note that for the studied concentration of shallow acceptors $N_{A0} \sim 5 \times 10^{18} \text{ cm}^{-3}$ the holes in GaAs are on the metallic side of the metal-insulator transition according to the Mott criterion [11,12]: $N_A^{1/3} a_H > 0.25$, where $a_H \approx 3 \text{ nm}$ is the Bohr radius of a hole bound to an acceptor [8]. Therefore, at first glance it is reasonable to assume that T_c corresponds to the temperature of the hole

gas. The temperature dependence of the PL step width is characterized by the thermal energy $k_B T_c$, which is plotted in the inset of Fig. 1(b) and can be well fitted with a linear dependence going through zero. The deviation from the fit around $T = 2$ K from the expected value of 0.2 meV is, as we suppose, due to the mesoscopic fluctuations of the energy gap within the laser excitation spot.

To identify the absorption edge, the PLE spectrum was measured at $T = 2$ and 8 K for a detection energy of $E_{\text{det}} = 1.467$ eV. Here, we observe a smooth and monotonous growth of PLE intensity with increasing photon energy from 1.49 to 1.51 eV. Thus, there is a drastic difference in the behavior of PL and PLE spectra. First, the sharp drop in the PL edge is significantly narrower than the smooth edge in the PLE, which is of the order of 10 meV. Second, in contrast to the PL data the PLE spectrum does not change when the temperature is increased from 2 to 8 K. If only the hole distribution would determine the spectrum's shape, we would expect the same step widths and temperature behavior in PL and PLE spectroscopy. Therefore, the drastic difference between PL and PLE spectra clearly indicates that the magnitude of T_c is determined not only by the temperature of the hole gas as it was proposed earlier. In what follows, we demonstrate that by measuring the Hanle effect and the time-resolved PL the spin lifetimes of the photoexcited electrons also show a sharp drop in their spectral dependence.

B. Hanle measurements

In order to measure the spin lifetime T_S of the photoexcited electrons in the vicinity of the step in the PL spectrum, we record the PL depolarization by an externally applied transverse magnetic field, i.e., we measure the Hanle effect at various detection energies around the PL step. Note that the resident holes are not spin polarized and do not contribute to the observed optical spin orientation. Application of the magnetic field in Voigt geometry causes a high-energy shift of the edgelike PL tail. For that reason we work in two different ranges of magnetic field strengths corresponding in one case to a relatively weak, negligible energy shift and in the other case to a non-negligible shift.

C. Voigt magnetic fields <0.5 T

In the first case, the standard Hanle method was used allowing for measurement of the spin lifetime $T_S = (1/\tau_S + 1/\tau)^{-1}$ through recording the PL depolarization curve as function of the external magnetic field and assessing the width of this curve. Here, τ_S is the spin relaxation time and τ is the electron lifetime, both of which limit the spin lifetime. The cw excitation by light with a photon energy of 1.55 eV and a pump density of 6 W cm^{-2} was periodically modulated between the two countercircular polarizations using a photoelastic modulator (PEM), operated at 50 kHz frequency. The degree of circular polarization (DCP) of the PL was measured by detecting the PL intensity in σ^+ polarization using a spectrometer with a resolution of ~ 1 nm, equipped with a photomultiplier. A two-channel photon counter synchronized with the PEM was used to measure the PL intensities $I_{\sigma^+}^{\sigma^+}$ and $I_{\sigma^+}^{\sigma^-}$, emitted during the periods of excitation with a polarization according to

the superscript. The subscript corresponds to the polarization state of the detection, which was kept constant. The DCP is calculated as

$$\rho^c = \frac{I_{\sigma^+}^{\sigma^+} - I_{\sigma^+}^{\sigma^-}}{I_{\sigma^+}^{\sigma^+} + I_{\sigma^+}^{\sigma^-}}. \quad (2)$$

It is equivalent to the degree of circular polarization measured for constant σ^+ excitation and variable σ^+/σ^- detection

$$\rho_c = \frac{I_{\sigma^+}^{\sigma^+} - I_{\sigma^+}^{\sigma^-}}{I_{\sigma^+}^{\sigma^+} + I_{\sigma^+}^{\sigma^-}}, \quad (3)$$

in the absence of circular dichroism, magnetic field induced circular polarization and dynamical nuclear polarization. This is applicable to our study where the DCP is measured in Voigt geometry, i.e., $\rho^c = \rho_c$. Therefore, in what follows we use ρ_c as a measure of the DCP.

The DCP was measured as a function of the magnetic field strength up to 0.4 T for a set of different detection energies at $T = 2$ K. Each of these data sets, shown in Fig. 2(a) by the symbols, was fitted by a zero-field centered Lorentzian with a vertical offset, which corresponds to an additional contribution with a very broad linewidth and an accordingly short T_S . The PL depolarization profiles show drastic changes when moving the detection energy across the steplike feature in the PL spectrum: the larger the detection energy is, the broader is the profile and the higher is the offset. At the very tail of the PL line, where the PL signal becomes small ($E > 1.495$ eV), the measured data are at a practically constant level. On the other hand, within the PL line ($E = 1.469$ eV) the PL depolarization curve is uniformly quite narrow.

From the Lorentzian fits to the data shown in Fig. 2(a) by the lines, the spin lifetime T_S of the relatively slow component corresponding to the narrow Hanle peak can be extracted using the equation

$$T_S = \frac{\hbar}{|g|\mu_B B_{1/2}}. \quad (4)$$

Here, μ_B is the Bohr magneton, \hbar is the Planck constant, $B_{1/2}$ is the Lorentzian half-width, and $|g| = 0.53$ is the electron g factor measured by time-resolved PL as shown below. The results of this analysis are displayed in Fig. 2(b), giving the spin lifetime as function of the detection energy in comparison with the PL spectrum at $T = 2$ K. Within the PL line, the spin lifetime is 250 ± 20 ps, but it becomes substantially shorter at $E > 1.49$ eV.

The same type of measurements were carried out also on the other sample with the acceptor concentration of $N_A = 3 \times 10^{18} \text{ cm}^{-3}$. Although its PL spectrum measured at 2 K is substantially narrower than that of the mainly studied sample due to the different levels of doping and the acceptor compensation with donors, it exhibits a similar high-energy edge. The corresponding PL depolarization curves and the extracted spin lifetimes T_S , together with the PL spectrum at $T = 2$ K, are shown in Figs. 2(c) and 2(d). This sample demonstrates a similarly sharp edge at the high-energy side of the PL spectrum and shows a qualitatively similar broadening of the PL depolarization curves in magnetic field for energies above this edge. The spin lifetimes drop from $T_S = 420$ to

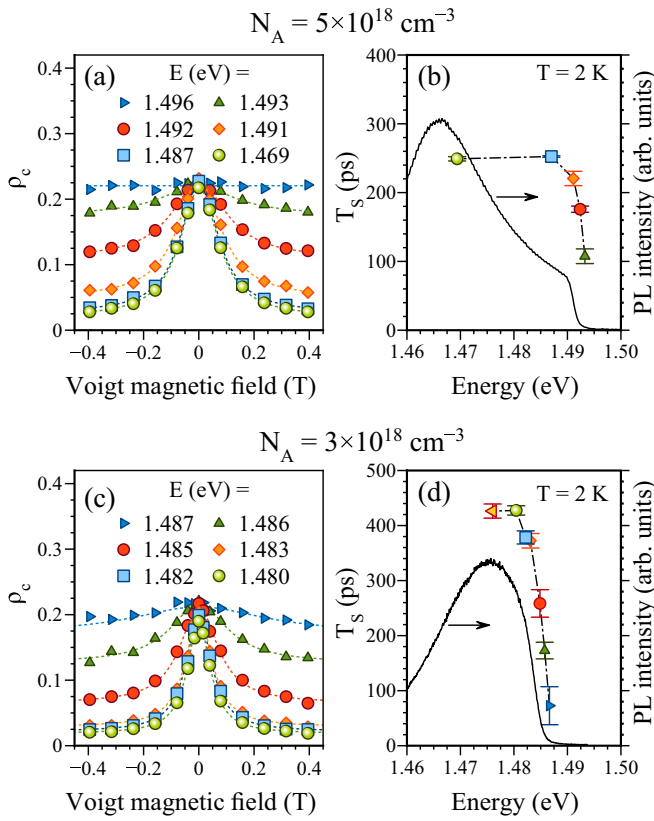


FIG. 2. PL depolarization measurements in the Voigt magnetic field range $B < 0.5$ T at $T = 2$ K. Data for the sample with the acceptor density $N_A = 5 \times 10^{18} \text{ cm}^{-3}$ are shown: (a) Set of PL depolarization curves measured as function of magnetic field strength for different detection energies (the symbols). Fits based on Eq. (4) are shown by the dashed lines. (b) Spectral dependence of the spin lifetime (the symbols with error bars). The data points are connected by the dashed-dotted line for clarity. For comparison, the PL spectrum at $T = 2$ K is shown by the solid line. The corresponding set of data for the sample with the acceptor density $N_A = 3 \times 10^{18} \text{ cm}^{-3}$ is displayed in (c) and (d).

70 ps at the edge. We concentrate in the following on the sample with the acceptor concentration $N_A = 5 \times 10^{18} \text{ cm}^{-3}$.

We note that experiments on similar structures at temperatures of 77 and 300 K revealed only a small difference in the halfwidth of the Hanle depolarization curves [8] between the short- and the long-wavelength spectral ranges [13]. At these temperatures, the carriers are hot and free and, as a result, the corresponding PL spectra exhibit no sharp high-energy edge.

D. Voigt magnetic fields > 0.5 T

Stronger magnetic fields are required to measure the short spin lifetimes, but they simultaneously cause a significant high-energy shift of the PL line. This can be seen from Figs. 3(a) and 3(b), where in (a) the high-energy edge of the PL spectrum measured at $T = 2$ K is shown for different magnetic fields, while (b) gives the high-energy shift of the edge as function of magnetic field. The high-energy shift is linear proportional to the field strength with the slope given

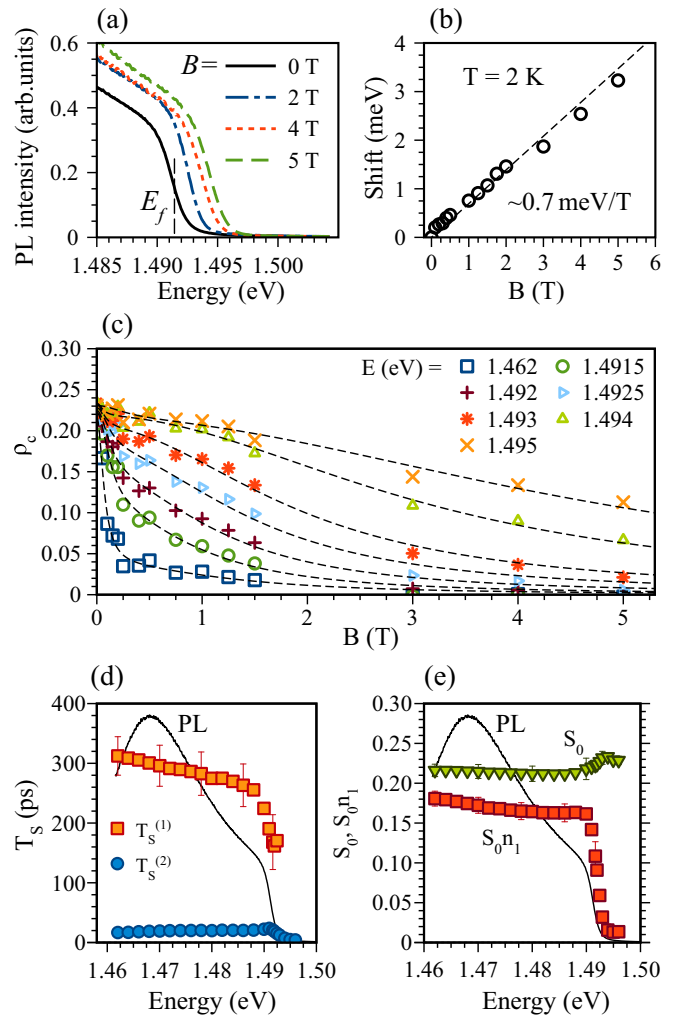


FIG. 3. Hanle effect in strong magnetic fields: (a) PL spectra around the high-energy edge for different magnetic field strengths. (b) Shift of the PL edge to higher energies as function of the magnetic field (circles), fitted with a B -linear dependence (dashed line). (c) Hanle PL depolarization curves obtained by the technique described in the text (the symbols) fitted by two Lorentzians (the dashed lines), according to Eq. (5). (d) Spin lifetimes of the two electron contributions: the localized electrons with $T_S^{(1)} \approx 280$ ps (the squares) and the free electrons with $T_S^{(2)} \approx 20$ ps (the circles). (e) Spectral dependence of the DCP, S_0 (the triangles), and of the relative contribution of the localized electrons $S_0 n_1$ to S_0 (squares), at $B = 0$. In (d) and (e) the error bars indicate the fitting error, the PL spectrum at $T = 2$ K is shown by the solid line.

by $\sim 0.7 \text{ meV/T}$. This slope is somewhat smaller than the one expected for the energy shift of an electron $\hbar\omega_c^e/2B \approx 0.86 \text{ meV/T}$, where ω_c^e is the electron cyclotron frequency. Due to this high-energy shift, the measurement of the PL depolarization curves around the PL edge becomes nontrivial using the standard Hanle technique. Instead, the PL depolarization by the magnetic field was studied through measuring PL spectra at $T = 2$ K. First, a set of PL spectra were recorded at different magnetic field strengths for σ^+ polarized excitation. The PL spectra were detected both for σ^+ and σ^- polarization from which DCP spectra were calculated using

Eq. (3). Then, the high-energy shift of these spectra was compensated to have the gap energy E_f at the same spectral position, independent of the magnetic field strength. Finally, cuts through this set of DCP spectra were taken for a number of fixed energies E , resulting in a set of data similar to the PL depolarization curves. Some of these data sets are shown in Fig. 3(c). At a certain energy, they were fitted with the following expression containing the contributions of two types of electrons:

$$\rho_c = S_0 \left[\frac{n_1}{1 + (g\mu_B T_S^{(1)} B / \hbar)^2} + \frac{1 - n_1}{1 + (g\mu_B T_S^{(2)} B / \hbar)^2} \right]. \quad (5)$$

Here, the $T_S^{(i)}$ are the spin lifetimes of the slow ($i = 1$) and fast ($i = 2$) decaying components, n_1 and $1 - n_1$ are the corresponding weights of these components, and S_0 is the total DCP at $B = 0$. The fitted values of $T_S^{(i)}$ and n_1 are shown as functions of energy in Figs. 3(d) and 3(e), respectively. We find good agreement of the spin lifetimes of the slow component measured in the two different field regimes.

The main result here is the identification of two types of electrons with substantially different spin lifetimes: $T_S^{(1)} \approx 280$ ps and $T_S^{(2)} \approx 20$ ps. Both types of electrons are observed across the whole PL spectral range. However, the PL line is mostly contributed by electrons having the long spin lifetime. At the high-energy PL edge, the weights of the two electron contributions de facto are exchanged, resulting in a dramatic shortening of the spin lifetime. Moreover, the spin lifetimes of both types of electrons experience a shortening at this edge. The sum of both contributions in the absence of a magnetic field, S_0 , also shown in Fig. 3(e), exhibits no significant changes with energy and does not drop below 0.21. This value is close to the maximum achievable DCP value of 25% in GaAs, which, in turn, indicates that the spin relaxation time τ_S is much longer than the electron lifetime τ . Based on the expression $S_0 = 0.25 / (1 + \tau / \tau_S)$, the following estimation can be done: $\tau_S > 5\tau$. Taking into account that the spin lifetime $1/T_S = 1/\tau + 1/\tau_S$, we conclude that T_S is likely limited by the electron lifetime τ . Using the procedure suggested by Paget [14] we estimate the characteristic time of the spin-exchange mechanism $\tau_{ex} \approx 1/\sigma v N > 1$ ns, for the electron concentration $N < 10^{13}$ cm $^{-3}$. Here, $\sigma \approx 10^{-11}$ cm $^{-2}$ is the used estimate for the scattering cross section of the free electron on a neutral donor, $v \approx 10^7$ cm/s is the average thermal electron velocity. τ_{ex} is substantially longer than the spin lifetimes $T_S^{(1)}$ and $T_S^{(2)}$ measured in our structure. Therefore, the exchange averaging is inefficient here.

E. Time-resolved photoluminescence

Time-resolved PL (TRPL) measurements using a streak camera were carried out in order to extract the electron lifetime τ . Here, the photoexcitation was done using picosecond laser pulses from a Ti:sapphire oscillator tuned to an energy of about 1.6 eV. The PL kinetics were detected spectrally resolved with a temporal resolution of about 20 ps and the data were averaged across a spectral window of 0.5 nm. The PL kinetics measured at $T = 2$ K for different energies E in absence of the external magnetic field are shown in Fig. 4(a). They reveal drastic changes in the decay when crossing the

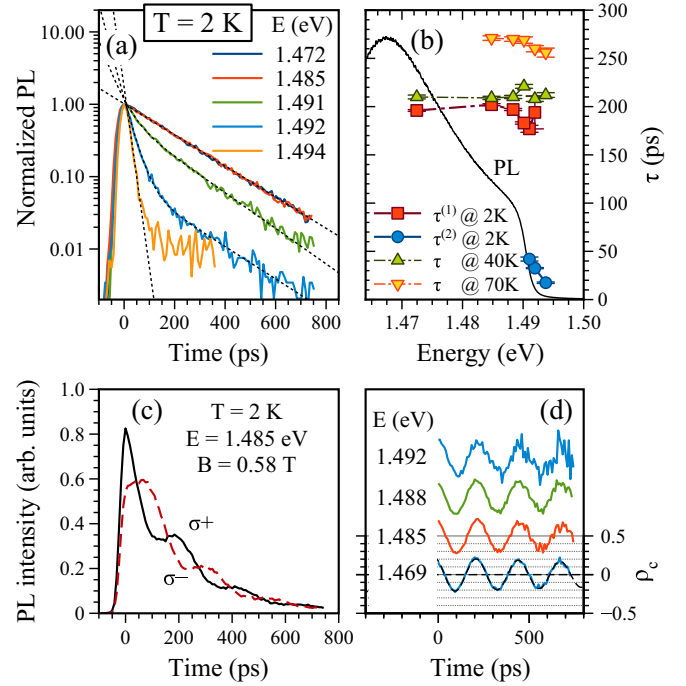


FIG. 4. Time-resolved PL measurements: (a) Normalized PL kinetics measured with a streak camera for different detection energies at $T = 2$ K (solid lines), fitted using monoexponential or biexponential decay forms (dashed lines). (b) Spectral dependence of the lifetime τ across the PL line, extracted from the fits to the PL kinetics, measured at $T = 2, 40,$ and 70 K; the PL spectrum for $T = 2$ K is shown by the solid line. (c) PL transients measured at $E = 1.485$ eV detection energy for $T = 2$ K at a Voigt magnetic field of $B = 0.58$ T. The excitation is σ^+ polarized, the detection is done in σ^+ and σ^- polarization, as shown by the solid and dashed lines, respectively. (d) Spin dynamics ρ_c detected for various detection energies (shifted vertically for clarity). The fit to the oscillations for $E = 1.469$ eV detection energy is shown by the dashed line.

high-energy PL edge. At the very edge ($E \gtrsim 1.49$ eV) the PL kinetics contain two components with different decay times of about 20 and 200 ps, while within the PL line ($E < 1.49$ eV) the fast component is absent. The PL kinetics were also measured at $T = 40$ and 70 K and exhibit purely monoexponential decays. The data were accordingly fitted with either a single-exponential or a biexponential function, the fitting results are displayed in Fig. 4(b). The shortest PL lifetime of $\tau^{(2)} \approx 20$ ps, measured at $T = 2$ K in the high-energy PL tail, is limited by the streak camera resolution. In the region $E < 1.49$ eV, the PL lifetime is independent of the detection energy. The fast component vanishes with rising temperature and the long PL lifetime increases from about $\tau^{(1)} = 200$ ps at $T = 2$ K to about 270 ps at 70 K.

Detection of the DCP $\rho_c(t)$ with temporal resolution makes it possible to measure the spin dynamics of the photoexcited carriers [15,16]. $\rho_c(t)$ was measured in an external magnetic field of $B = 0.58$ T, applied in Voigt geometry. The excitation was done with σ^+ polarized pulses and the PL kinetics were measured both in σ^+ and σ^- polarizations ($I_{\sigma_{\pm}^+}$). These kinetics are shown in Fig. 4(c) for $E = 1.485$ eV detection energy. The resulting DCP transients calculated using Eq. (3)

are plotted in Fig. 4(d) for a set of detection energies. All traces manifest oscillations, which can be fitted well with $\rho_c = A \cos(\Omega_L t + \phi_0) \exp(-t/T_2^*)$. Here, $\Omega_L = g\mu_B B/\hbar$ is the Larmor frequency of the electron spin precession, A is the initial DCP, g is the carrier g factor, T_2^* is the spin dephasing time, and ϕ_0 is a phase offset. From these fittings we obtain $A = 0.23 \pm 0.01$, which is close to the maximal possible DCP value $\rho_c(B=0) = 0.25$. The obtained value for the g factor 0.53 ± 0.01 slightly deviates from that of the electron measured in pure GaAs [17,18], $|g| = 0.44$, which can be caused by the band-gap renormalization [19,20] due to the hole-hole interactions or by disorder. The obtained spin dephasing time of $T_2^* = 2.0 \pm 0.7$ ns is limited by the electron g -factor dispersion of $\Delta g = 0.006$. We have checked this by the time-resolved Faraday rotation measurements described in the Appendix.

We compare the results of our measurements with the spin relaxation times obtained from optical orientation and Hanle measurements by Miller *et al.* [6] and Zerouati *et al.* [21] where shorter times in the range from 0.2 to 1 ns were reported. Quantitative estimation of the spin relaxation time τ_S using the optical orientation method is difficult when $\tau \ll \tau_S$. In this case, the halfwidth of the Hanle curve is defined by the carrier lifetime τ , while the degree of polarization in zero field reaches 25%. Then, the time τ_S is estimated from the deviation from these 25%. This deviation, however, might be caused by various reasons, e.g., spin relaxation during thermalization, variation of the selection rules for optical transition due to deformation, etc. We assume that this is the reason of the discrepancy between our measurements and the values obtained by Miller and Zerouati. Therefore, our TRPL measurements of τ_S independent of the polarization degree being close to 25% are more reliable.

III. DISCUSSION

The most striking result here is the steplike spectral dependence of the halfwidth $B_{1/2}$ of the Hanle depolarization curve of the PL and its correlation with the sharp edge in the PL spectrum with a width $k_B T_c < 1$ meV (at $T = 2$ K) in a strongly disordered semiconductor. Indeed, for a typical compensation degree of 0.1, the density of ionized donors and acceptors reaches the value $N_{D^+} = N_{A^-} \sim 5 \times 10^{17} \text{ cm}^{-3}$. This means that the characteristic spatial potential fluctuations of the charged impurities amount to $\mathcal{E}_{fl} \sim (N_{D^+})^{1/3} e^2/\kappa \approx 5$ meV, where e is the electron charge and $\kappa \approx 13$ is the static dielectric constant of GaAs [2]. This estimate corresponds well to the characteristic spectral broadening of the low-energy flank of the PL spectrum of about 10 meV [Fig. 1(a)], formed by the Urbach tail of localized states [22]. Thereby, the broadening of the bottom of the conduction band (as well as the top of the valence band) is much larger than $k_B T_c$.

Olego and Cardona suggested that the high-energy edge in the PL spectrum is determined by the Fermi level delimiting the occupied hole states from the unoccupied ones [5]. However, the momentum \mathbf{k} in such a disordered system is not a good quantum number anymore and the optical transitions are not purely vertical in the \mathbf{k} space [23,24]. Thus, the position of the step is not well defined and is expected to be given by the inhomogeneous broadening of the conduction band edge.

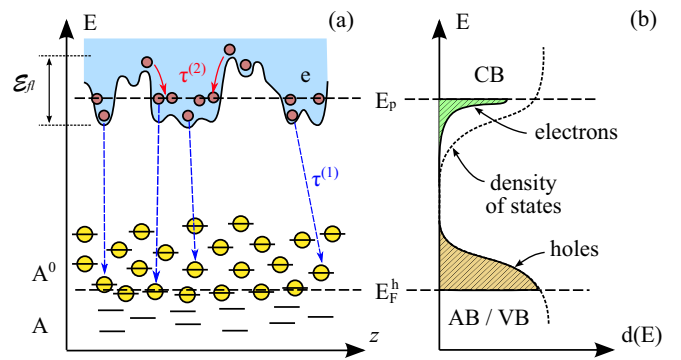


FIG. 5. Energy states and optical transitions in a heavily p -doped GaAs crystal. (a) Possible optical transitions in the crystal. The potential landscape is shown by the curved line about the E_p level. Notations: e are electrons (the small circles); A_0 are the neutral acceptors; A^- are the ionized acceptors. The red solid and blue dashed arrows indicate the fast energy relaxation of the delocalized electrons ($\tau^{(2)} \approx 20$ ps) and the slow recombination of the localized electrons ($\tau^{(1)} \approx 280$ ps) with the equilibrium holes, respectively. \mathcal{E}_{fl} is the characteristic energy scale of the potential fluctuations in the conduction band. (b) Density of states $d(E)$ (the dotted line) and ranges of occupied states (the shaded areas). E_F^h is the Fermi level of the holes in the acceptor or the valence band (AB/VB); E_p is the percolation threshold for the electrons in the conduction band (CB).

Also, the PLE spectrum [Fig. 1(c)] displays a smooth spectral behavior and does not demonstrate a sharp steplike edge as observed in the PL spectrum, despite the Fermi level of the holes.

Our hypothesis is based on a sharp edge in the distribution of nonequilibrium conduction band electrons which appears in the vicinity of the percolation threshold. The threshold is located in the empty conduction band [2,3] at the energy level E_p , separating the localized electron states from the extended electron states. The electron states with energies $E < E_p$ are spatially localized, while those with $E > E_p$ are delocalized over the crystal. The photoexcited electrons, which undergo rapid energy relaxation by emitting acoustic phonons, reach the energy level E_p and quickly get trapped at this level, forming a steplike spectral distribution $n(E - E_p)$, as illustrated in Fig. 5(b). The energy relaxation by phonon emission occurs in small energy portions of $\hbar\omega_q = \hbar sq \leq k_B T \approx 0.2$ meV because the characteristic electron momentum transferred to the phonons is $q \sim 1/L \sim 10^6 \text{ cm}^{-1}$. Here, $s \approx 3 \times 10^5 \text{ cm s}^{-1}$ is the speed of sound in GaAs and $L \sim (N_{D^+})^{-1/3} \sim 10$ nm is the characteristic length scale of the potential fluctuations of the impurities. The characteristic energy relaxation time corresponds to the short decay time of $T_S^{(2)} = 20$ ps, measured using the Hanle effect and TRPL. Note that the step width in the electron distribution around $E = E_p$ increases with increasing temperature. This is because the trapped electrons with energy $E < E_p$ can get thermally activated into the higher-energy states with $E > E_p$ due to absorption of an acoustic phonon with characteristic energy $k_B T$, as discussed in the phenomenological model presented in Refs. [23,24].

The energy relaxation rate slows down drastically at $E \leq E_p$ since the changes in electron energy due to the phonon emission require changes of the electron position. Therefore, the lifetime of the electrons below the percolation threshold becomes significantly longer and is limited now by their

radiative recombination with the holes on the acceptors, leading to an extension of the decay time to $T_S^{(1)} = 280$ ps. As a result, the recombination of the electrons below the level E_p with holes causes the low-energy PL line characterized by a long radiative recombination time. On the contrary, the high-energy PL edge is due to the recombination of hot electrons with $E > E_p$, whose lifetime is limited by the energy relaxation to 20 ps.

From these considerations it follows that the sharpness of the high-energy PL spectrum edge is determined by both the sharp edge in the Fermi-Dirac distribution ($\sim k_B T$) of the holes and the steplike energy distribution of the electrons in the vicinity of the percolation level with characteristic width of ~ 0.2 meV in the limit of low temperatures. The dependence of the spectral distribution $n(E - E_p)$ below the percolation threshold, i.e., for $E < E_p$, is difficult to determine from our measurements since it is masked by the wide distribution of the equilibrium holes on the acceptors. It can be narrower as compared to hole bandwidth since the trapped electrons require tunneling between the localization sites during relaxation down to more strongly localized states, and therefore they can not reach all possible low-energy localization centers before recombination with holes. The approximate energy diagram is illustrated in Fig. 5(b), where the line denotes the smooth density of states and the hatched areas denote the occupied states.

Our study points to universal method for high-precision measurements of the percolation level of electrons in the conduction band, once the Fermi level of the holes with respect to vacuum has been identified independently, e.g., by photoemission measurements. Our results show that the photon energy corresponding to the sharp step in the low-temperature PL spectrum corresponds to $E_f = E_p - E_F^h$ where the percolation threshold in the conduction band E_p and the Fermi energy in the valence band E_F^h are taken with respect to some reference energy level, e.g., the vacuum. Evaluation of E_F^h through photoemission measurements and E_f from PL spectra [see Fig. 1(b)] allows one to determine the value of E_p . Note that transport measurements are not relevant for evaluation of the percolation level in the conduction band for strongly doped p -type semiconductors.

There is one question that has been discussed in literature starting from the middle of the last century, namely, the question of the location of the hole Fermi level in heavily p -doped GaAs: Is it located inside the valence band or within the band gap [25]? Different opinions have been expressed, based on absorption and PL measurements in GaAs with varying impurity concentrations [5,26]. From our experiments it is difficult to conclude about the exact location of the hole Fermi level. This is, however, not critical for understanding the physics responsible for the steplike energy distribution of the electrons as studied here.

IV. CONCLUSIONS

We have studied the electronic processes occurring near the Fermi-type tail of the PL spectrum of a strongly p -doped GaAs crystal using a large variety of optical techniques. We demonstrate a sharp steplike dependence in the energy distribution of nonequilibrium photoexcited electrons in the

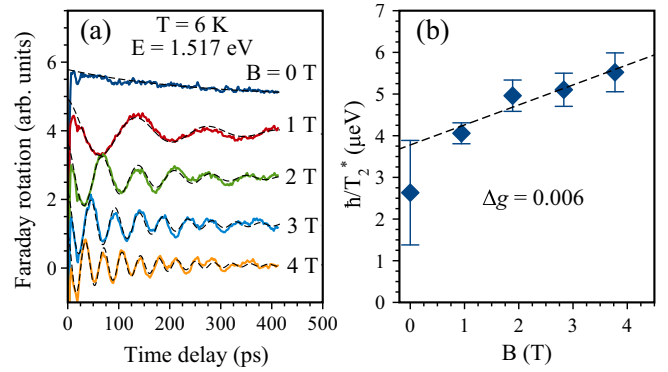


FIG. 6. Time-resolved Faraday rotation for $T = 6$ K at $E = 1.517$ eV detection energy: (a) Faraday rotation signals at different Voigt magnetic fields (the solid lines) with corresponding fits (the dashed lines). (b) Extracted values for the spin dephasing rate \hbar/T_2^* (the symbols) as function of the magnetic field, shown together with a B -linear fit function, from which a g -factor spread $\Delta g = 0.006$ is obtained.

vicinity of the percolation energy level, which separates free and localized conduction band states. The presence of the sharp step in the distribution of nonequilibrium electrons is a nontrivial fact due to the high disorder in the crystal lattice and the absence of translation symmetry. In addition to the well-defined percolation energy level it requires abrupt changes in the energy relaxation time of photoexcited electrons which is unambiguously supported by Hanle effect and time-resolved measurements of spin-polarized electrons. As a result, the spectral profile of the high-energy photoluminescence edge and its sharpness are determined not only by the hole distribution, but also by the energy distribution of the conduction band electrons, which exhibit a steplike behavior. It might be interesting to go to sub-Kelvin temperatures and spatially resolved microscopy in order to disclose the physics affecting the sharpness of the PL spectral edge in more detail.

ACKNOWLEDGMENTS

The authors thank N. E. Kopteva for useful discussions and assistance in spectroscopic experiments, A. S. Terekhov for providing the samples. I.A.A., D.R.Y., and M.B. acknowledge the Deutsche Forschungsgemeinschaft for financial support through the International Collaborative Research Centre TRR160 (Project No. A3). S.V.P. thanks the Russian Foundation for Basic Research for partial financial support (Research Grant No. 19-52-12046 NNIO_a) and acknowledges St. Petersburg State University (Grant No. 51125686).

APPENDIX: TIME-RESOLVED FARADAY ROTATION

Time-resolved pump-probe Faraday rotation was applied for measuring accurately the Δg dispersion value of the g factor. For this purpose, Voigt magnetic fields in the range 0–4 T were applied to the sample at $T = 6$ K. Optical pumping and probing were done with two degenerate picosecond pulse trains, generated by a Ti:sapphire laser. The delay between the pump and probe pulses was varied by an optical delay line. The circular polarization of the pump

pulse was modulated between σ^+ and σ^- using a PEM operated at 50 kHz frequency. The rotation angle of the linear polarization of the probe pulse was measured in transmission geometry at this modulation frequency, using a detection scheme with a polarized beam splitter and a balanced photodetector.

The transients of Faraday rotation measured at $E = 1.517$ eV excitation energy for different magnetic fields are shown in Fig. 6(a). In the absence of a magnetic field, a monotonic decay with a time constant of $T_0 \approx 250$ ps is observed. This value agrees with the PL decay time measured on the high-energy flank of the PL line (~ 200 ps at $E = 1.492$ eV) and, thus, corresponds to the recombination time of the photoexcited electrons.

The other transients for $B > 0$ are fitted with exponentially decaying harmonic functions. This gives us the magnetic-field-dependent decay time T_2^* , shown in Fig. 6(b) as the spin dephasing rate \hbar/T_2^* . At $B > 0$ this rate can be approximated with a linear B dependence $\hbar/T_2^* = \hbar/T_0 + \sqrt{2}\mu_B\Delta gB$, from which the value of the g -factor dispersion $\Delta g = 0.006$ is obtained. Using this value we estimate a spin dephasing time of about 2 ns at $B = 0.58$ T. This value agrees with the T_2^* (also ≈ 2 ns) obtained from the TRPL experiment. Thus, we conclude that τ_S is at least several nanoseconds in the studied sample. We confirm also that the fitted electron g -factor value $g \approx 0.50$ is in agreement with the TRPL measurements. Experimentally, we checked that the g factor does not depend on temperature in the range 6–25 K.

-
- [1] O. Madelung and B. Taylor, *Introduction to Solid-State Theory* (Springer, Berlin, 1996).
- [2] B. I. Shklovskii and A. L. Efros, *Electronic Properties of Doped Semiconductors* (Springer, Berlin, 1984).
- [3] P. W. Anderson, Absence of diffusion in certain random lattices, *Phys. Rev.* **109**, 1492 (1958).
- [4] K. v. Klitzing, G. Dorda, and M. Pepper, New Method for High-Accuracy Determination of the Fine-Structure Constant Based on Quantized Hall Resistance, *Phys. Rev. Lett.* **45**, 494 (1980).
- [5] D. Olego and M. Cardona, Photoluminescence in heavily doped GaAs. I. Temperature and hole-concentration dependence, *Phys. Rev. B* **22**, 886 (1980).
- [6] R. C. Miller, D. A. Kleinman, W. A. Nordland, Jr., and R. A. Logan, Electron spin relaxation and photoluminescence of Zn-doped GaAs, *Phys. Rev. B* **23**, 4399 (1981).
- [7] P. Y. Yu and M. Cardona, *Fundamentals of Semiconductors: Physics and Materials Properties*, 3rd ed. (Springer, Berlin, 2005), p. 354.
- [8] F. Meier and B. P. Zakharchenya, *Optical Orientation* (Elsevier, Amsterdam, 1984).
- [9] M. K. Hudait, P. Modak, K. S. R. K. Rao, and S. B. Krupanidhi, Low temperature photoluminescence properties of Zn-doped GaAs, *Mater. Sci. Eng. B* **57**, 62 (1998).
- [10] M. Kucera and J. Novák, Optical characterization of gallium antimonide highly doped with manganese, *J. Phys. Chem. Solids* **67**, 1724 (2006).
- [11] N. F. Mott and E. A. Davis, *Electronic Processes in Non-Crystalline Materials* (Oxford University Press, New York, 1979).
- [12] A. Ferreira da Silva, I. Pepe, Bo E. Sernelius, C. Persson, R. Ahuja, J. P. de Souza, Y. Suzuki, and Y. Yang, Electrical resistivity of acceptor carbon in GaAs, *J. Appl. Phys.* **95**, 2532 (2004).
- [13] R. I. Dzhiyev, B. P. Zakharchenya, R. R. Ichkitidze, K. V. Kavokin, and P. E. Pak, Spectral dependence of the Hanle effect due to diffusion of optically oriented electrons in p -type semiconductors, *Fiz. Tverd. Tela* (St. Petersburg) **35**, 2821 (1993) [*Phys. Solid State* **35**, 1396 (1993)].
- [14] D. Paget, Optical detection of NMR in high-purity GaAs under optical pumping: Efficient spin-exchange averaging between electronic states, *Phys. Rev. B* **24**, 3776 (1981).
- [15] A. P. Heberle, W. W. Rühle, and K. Ploog, Quantum Beats of Electron Larmor Precession in GaAs Wells, *Phys. Rev. Lett.* **72**, 3887 (1994).
- [16] I. A. Akimov, R. I. Dzhiyev, V. L. Korenev, Y. G. Kusrayev, E. A. Zhukov, D. R. Yakovlev, and M. Bayer, Electron-spin dynamics in Mn-doped GaAs using time-resolved magneto-optical techniques, *Phys. Rev. B* **80**, 081203(R) (2009).
- [17] C. Weisbuch and C. Hermann, Optical detection of conduction-electron spin resonance in GaAs, $\text{Ga}_{1-x}\text{In}_x\text{As}$, and $\text{Ga}_{1-x}\text{Al}_x\text{As}$, *Phys. Rev. B* **15**, 816 (1977).
- [18] M. Oestreich and W. W. Rühle, Temperature Dependence of the Electron Landé g Factor in GaAs, *Phys. Rev. Lett.* **74**, 2315 (1995).
- [19] E. L. Ivchenko, *Optical Spectroscopy of Semiconductor Nanostructures* (Alpha Science International, Oxford, 2005).
- [20] L. M. Roth, B. Lax, and S. Zwerdling, Theory of optical magneto-absorption effects in semiconductors, *Phys. Rev.* **114**, 90 (1959).
- [21] K. Zerrouati, F. Fabre, G. Bacquet, J. Bandet, J. Frandon, G. Lampel, and D. Paget, Spin-lattice relaxation in p -type gallium arsenide single crystals, *Phys. Rev. B* **37**, 1334 (1988).
- [22] J. I. Pankove, *Optical Processes in Semiconductors* (Prentice Hall, Englewood Cliffs, New Jersey, 1971).
- [23] A. Y. Shik, *Electronic Properties of Inhomogeneous Semiconductors* (Gordon & Breach, Amsterdam, 1995).
- [24] A. P. Levanyuk and V. V. Osipov, Edge luminescence of direct-gap semiconductors, *Sov. Phys. Usp.* **24**, 187 (1981).
- [25] J. Pankove, Absorption edge of impure gallium arsenide, *Phys. Rev.* **140**, A2059 (1965).
- [26] D. Zhang, K. Radhakrishnan, S. Yoon, and Z. Han, Photoluminescence in degenerate p -type GaAs layers grown by molecular beam epitaxy, *Mater. Sci. Eng. B* **35**, 449 (1995).